HHS Public Access

Author manuscript

Clin Cancer Res. Author manuscript; available in PMC 2016 April 15.

Published in final edited form as:

Clin Cancer Res. 2015 April 15; 21(8): 1925–1934. doi:10.1158/1078-0432.CCR-14-2031.

Anti-S1P antibody as a novel therapeutic strategy for VEGFR TKI resistant renal cancer

Liang Zhang[#1], **Xiaoen Wang**[#1,2], **Andrea J. Bullock**[1], **Marcella Callea**[3], **Harleen Shah**[4], **Jiaxi Song**[3], **Kelli Moreno**[5], **Barbara Visentin**[5], **Douglas Deutschman**[6], **David C. Alsop**[2], **Michael B. Atkins**[7], **James W. Mier**[1], **Sabina Signoretti**[3], **Manoj Bhasin**[4], **Roger A. Sabbadini**[5], and **Rupal S. Bhatt**[1,$]

[1]Division of Hematology-Oncology and Cancer Biology, Beth Israel Deaconess Medical Center, Harvard Medical School, 330 Brookline Avenue, Boston, Massachusetts, 02215, United States of America

[2]Department of Radiology, Beth Israel Deaconess Medical Center, Harvard Medical School, 330 Brookline Avenue, Boston, Massachusetts, 02215, United States of America

[3]Department of Pathology, Brigham and Women's Hospital, Harvard Medical School, 75 Francis Street, Boston, Massachusetts, 02115, United States of America

[4]Division of Interdisciplinary Medicine and Biotechnology, and Genomics and Proteomics Center, Beth Israel Deaconess Medical Center, Harvard Medical School, 330 Brookline Avenue, Boston, Massachusetts, 02215, United States of America

[5]Lpath Inc., 4025 Sorrento Valley Blvd. San Diego, CA, 92121, United States of America

[6]Department of Biology, San Diego State University, 5500 Campanile Dr. San Diego, CA. 92182-4614, United States of America

[7]Departments of Oncology and Medicine, Georgetown-Lombardi Comprehensive Cancer Center, 3970 Reservoir Road, NW, Washington, DC. United States of America

[#] These authors contributed equally to this work.

Abstract

Purpose—VEGFR2 tyrosine kinase inhibition (TKI) is a valuable treatment approach for patients with metastatic RCC. However, resistance to treatment is inevitable. Identification of novel targets could lead to better treatment for both patients with TKI naïve or resistant RCC.

Experimental design—In this study, we performed transcriptome analysis of VEGFR TKI resistant tumors in a murine model and discovered that the SPHK/S1P pathway is upregulated at the time of resistance. We tested S1P pathway inhibition using an anti-S1P mAb (sphingomab), in two mouse xenograft models of RCC, and assessed tumor SPHK expression and S1P plasma levels in patients with metastatic RCC.

[$]Corresponding Author: Rupal S. Bhatt, MD/PhD, Division of Hematology-Oncology and Cancer Biology, Beth Israel Deaconess Medical Center, 330 Brookline Avenue, Boston, MA 02215. USA Phone number: 617-735-2062 Fax number: 617-735-2060 RBHATT@BIDMC.HARVARD.EDU.

Conflicts of interest: RB received a grant from Lpath Inc. to support a portion of this study.

Results—Resistant tumors expressed several hypoxia regulated genes. The SPHK1 pathway was among the most highly upregulated pathways that accompanied resistance to VEGFR TKI therapy. SPHK1 was expressed in human RCC, and the product of SPHK1 activity, S1P, was elevated in patients with metastatic RCC suggesting that human RCC behavior could, in part, be due to over-production of S1P. Sphingomab neutralization of extracellular S1P slowed tumor growth in both mouse models. Mice bearing tumors that had developed resistance to sunitinib treatment also exhibited tumor growth suppression with sphingomab. Sphingomab treatment led to a reduction in tumor blood flow as measured by MRI.

Conclusions—Our findings suggest that S1P inhibition may be a novel therapeutic strategy in patients with treatment naïve RCC and also in the setting of resistance to VEGFR TKI therapy.

Keywords

Renal cell carcinoma; sphingosine kinase 1; sphingosine -1- phosphate; VEGFR

Introduction

Renal cell carcinoma (RCC) is the seventh most common cancer among US men and ninth among US women(1). Twenty percent of patients present with locally advanced disease and an additional 30% eventually develop distant metastases(2,3). Traditionally, treatment for metastatic RCC has been limited. Standard chemotherapeutic agents have been largely ineffective and cytokine-based treatments with interleukin-2 (IL-2) or interferon-α (IFNα) benefit only a small proportion of patients.

A major advance in the treatment of advanced RCC over the last decade has been the development and approval of several antitumor agents that function primarily as inhibitors of vascular endothelial growth factor (VEGF)-driven angiogenesis or the mammalian target of rapamycin (mTOR). The tyrosine kinase inhibitors (TKIs), sunitinib, sorafenib, axitinib, and pazopanib, have shown single agent activity in patients with metastatic RCC likely based on their ability to block VEGF receptor-2 (VEGFR2)(4–7). In the targeted therapy era, five year overall survival has been improving from about 10% to 20-25% but overall survival is still only in the range of 29 months (8,9). Inhibitors of the mTOR pathway, temsirolimus and everolimus, have also shown activity in patients with metastatic RCC leading to their approval in subsets of patients with advanced RCC(10,11). Despite these exciting results, there are few if any complete or durable responses to these agents and tumors develop resistance to all of these treatments usually within 4-12 months. Thus, there is still a critical need for the development of new treatment strategies for patients with this disease.

Sphingosine-1-phosphate (S1P) is a bioactive lipid with both tumorigenic and angiogenic activity (12). Sphingolipids comprise a group of intracellular and extracellular signaling molecules that have effects on cell proliferation, chemotaxis, and cytoskeletal stabilization. S1P was initially identified for its role in wound healing and inflammation where it acts via interaction with a series of G protein-coupled receptors. Previous studies have shown that S1P is a pro-angiogenic growth factor responsible for the development of capillary tube formation *in vitro* as well as vascular networks *in vivo*(13,14). In addition, S1P has

oncogenic functions including tumor cell growth promotion by inhibition of apoptosis and enhancing metastasis of human cancer cell lines by promoting motility and invasion (15–17). Sphingosine-kinase-1 (SPHK1) activity catalyzes the production of S1P. A number of studies have shown overexpression of SPHK1 in human solid tumors including breast, colon, lung, ovary, gastric, endometrial, and rectal cancers (18–25). Moreover, increased expression of SPHK1 is correlated with decreased survival in patients with several forms of cancer (18,20,21,23,26,27). It has been proposed that upregulation of the oncogene, *SPHK1*, and the resulting release of S1P into the tumor microenvironment could represent an important way cancer cells become resistant to treatment(28,29).Because of S1P's anti-apoptotic, pro-metastatic and angiogenic properties, the S1P signaling system is the target of anti-cancer drug discovery efforts, particularly in the setting of treatment resistance(17). One potential therapeutic intervention point is to block extracellular S1P with the use of specific anti-S1P mAbs(12,14,30). In this report, we demonstrate that the murine anti-S1P mAb, sphingomab, can slow tumor growth in treatment naïve murine RCC xenograft models. In addition, VEGFR TKI treatment leads to upregulation of the SPHK1 pathway and S1P inhibition exhibits activity after VEGF TKI treatment. We also demonstrate for the first time that RCC patients have elevated S1P levels in plasma and SPHK expression in tumor tissue, suggesting that the behavior of human RCC could, in part, be due to overproduction of S1P.

Materials and Methods

Tumor xenograft induction

Female athymic nude/beige mice (Charles River Laboratories, MA) were used for subcutaneous xenograft tumor models as described previously(31). All experiments were approved by the Beth Israel Deaconess Medical Center Institutional Animal Care and Use Committee. To establish RCC tumor xenografts, 1×10^7 786-O or A498 tumor cells were prepared and injected subcutaneously into the flanks of 6-8 week old mice. To ensure a consistent size at the outset of treatment, tumors were measured with calipers daily once they reached a diameter of 3-5 mm. Sunitinib (additive-free, 53.6 mg/kg) was administered 6 out of 7 days per week by gavage beginning when the tumors had grown to a diameter of 12 mm as previously described(31,32). Treated and control tumors were again measured daily during therapy. Mice were sacrificed when the tumors reached 20 mm in long axis. Resistance was defined as the time required for tumors to show the smallest measurable increase in diameter (2mm in long axis). This increase also roughly approximates the clinical definition of resistance (20% increase in long axis of tumors by RECIST criteria) (31,33).

Quantitative real-time PCR analysis

Quantitative real-time PCR (qt-RT-PCR) analysis was performed by a two-step process, a 15-cycle preamplification step (AmpliTaq® DNA Polymerase Kit; Applied Biosystems Inc., Foster City, CA, USA) followed by measurement of mRNA with an ABI PRISM 7900HT Sequence Detection System. For the measurement of mRNA levels *SPHK1*, primers were custom designed and ordered from IDT (San Diego, CA). The sequences of the primers are: forward 5’-CTTGCAGCTCTTCCGGAGTC-3’, reverse 5’-GCTCAGTGAGCATCAGCGTG-3’.

Gene Expression Analysis

The transcriptional profile of tumor response to drugs was characterized by oligonucleotide microarray analysis using the human U133 PLUS 2.0 Affymetrix GeneChip, according to previously described protocols for total RNA extraction and purification, cDNA synthesis, in vitro transcription reaction for production of biotin-labeled cRNA, hybridization of cRNA with U133 PLUS 2.0 Affymetrix gene chips, and scanning of image output files. The differentially expressed genes were identified by group-wise comparison of untreated vs. VEGFR TKI resistant samples after preprocessing and normalization of data. Differentially expressed genes were identified using a linear model for microarray analysis(34). The microarray data was deposited in the NCBI/GEO database (accession number GSE64052). *Limma* estimates the differences between Control and Resistance by fitting a linear model and using an empirical Bayes method to moderate standard errors of the estimated log-fold changes for expression values from each probe set. The differentially expressed probes were identified on the basis of absolute fold change (Fold Change >1.5) and P value (P value <0. 05).

Interactive Network analysis

To decipher the interaction among commonly differentially expressed genes we performed interactive network analysis. The interactive network was generated using known Protein-Protein, Protein-DNA, co-expression and Protein-RNA interactions. The interaction information was obtained using literature search and publically available databases. The interaction networks were analyzed using the bottleneck algorithm(35) to identify top master regulator genes involved in the stability of the resistance network.

Human plasma analysis

Human plasma was collected from patients under a protocol approved by our institutional review board at Dana Farber/Harvard Cancer Center. Plasma was collected from RCC patients with known metastatic disease or from healthy volunteers. Sodium Citrate tubes were used for plasma collection. S1P levels in human plasma samples were determined by a competitive ELISA using a biotinylated anti-S1P antibody and a S1P-coating conjugate covalently linked to BSA(30). High binding plates were coated with 1g/mL S1P-bovine serum albumin (BSA) conjugate in carbonate buffer for 1 hr at 37°C, and then blocked overnight in 1% fatty acid free BSA/ (phosphate buffered saline) PBS solution. For the primary incubation, S1P standards (1-2μM) or the human plasma samples were opportunely diluted in delipidated human serum (DHS), pre-mixed with 0.8 μg/mL biotinylated anti-S1P antibody and then added to the S1P-BSA coated plates for 1hr at room temperature. Plates were washed 4 times in 1X PBS, and then the biotinylated antibody competing for S1P coated on the plate against the S1P present in the biological samples was revealed by HRP streptavidin system (final dilution 1:60000, Jackson Immunoresearch) secondary detection. Plates were finally developed with TMB (Invitrogen), blocked with 0.1 M H_2SO_4 and optical densities were read at 450 nm using a Thermo Multiskan (Thermo Scientific). S1P levels in human plasma samples were then extrapolated from S1P standard curves plotted on GraphPad for analysis.

Tumor perfusion imaging

Tumor perfusion imaging with arterial spin-labeled MRI (ASL MRI) was performed as previously described(32,33,36). In briefly, mice were anaesthetized and imaged with a 3-cm surface coil on a 3.0 T whole-body clinical MRI scanner. A single transverse slice of ASL imaging was carefully positioned at the center of the tumor, which was marked on the skin with a permanent marker pen for follow-up MRI studies. Each ASL image was obtained with a single-shot fast spin echo sequence by using a background suppressed and flow-sensitive alternating inversion-recovery strategy. Using standard methods to quantify tumor perfusion(37), a region of interest was drawn around the peripheral margin of the tumor on the reference image that was then copied to the perfusion image. The mean blood flow for the tumor tissue within the region of interest was derived.

Immunohistochemistry

Formalin-fixed paraffin-embedded (FFPE) tissue blocks from 12 primary clear cell renal cell carcinoma (ccRCC) patients were retrieved. One primary ccRCC was paired with a corresponding lung metastasis. Areas of primary tumors containing low (G1-G2) and high (G3-G4) Fuhrman nuclear grade (FNG) were selected for the analysis. Immunohistochemistry was performed on four micron-thick, FFPE tumor sections, which were initially deparaffinized, rehydrated and heated with a pressure cooker to 125°C for 30 seconds in citrate buffer for antigen retrieval and then incubated with peroxidase (Dako #S2003, Carpinteria, CA) and protein blocking reagents (Dako #X0909), respectively, for 5 minutes. Sections were then incubated with an anti-SPKH1 antibody (1:500, Abcam #ab16491) for 1 hour at room temperature followed by incubation with the Dako EnVision+ System HRP labeled polymer anti-rabbit (Dako #K4011) for 30 minutes(26,38). All sections were developed using the DAB chromogen kit (Dako K3468) for 2 minutes and then lightly counterstained with hematoxylin. A case was considered positive if any positivity in tumor cells was detected.

Statistics

Differences in tumor length and volume were analyzed with ANOVA. Significant differences were assessed with Fisher's Least Significant Difference test.

Results

Sphingosine kinase is upregulated at the time of VEGFR TKI resistance

We have previously shown that VEGFR TKI treatment initially induces rapid tumor devascularization. Then as tumors develop resistance to treatment we note resumption of blood flow and tumor growth despite continued therapy (31,36). A murine VHL deficient RCC xenograft model (786-O) was treated with the VEGFR TKI, sorafenib. Transcriptome analysis of these tumors was performed and is shown in Figure 1. *SPHK1* was among the genes showing significant upregulation in the resistant tumors. In addition to *SPHK1*, which has been shown to be regulated by hypoxia and HIF, several other known HIF regulated genes were identified in the array analysis. These include angiopoietin like 4 (ANGPTL4),

HIF2 (HIG2), and C-X-C chemokine receptor type 4 (CXCR4). RT-PCR was also performed to validate the SPHK1 increase (Figure 1b, P=0.005).

To further explore the importance of SPHK1 regulation, we also analyzed transcriptome profiles from another VHL deficient RCC xenograft model, A498, treated with sorafenib. Additionally, the 786-O tumor model transcriptome was also performed after treatment with sunitinib. Seventy-five genes were significantly differentially expressed in all 3 treatment groups after VEGFR TKI treatment. These 75 genes were then used for systems biology analysis using interactive network analysis to identify the master regulators involved in resistance to VEGFR TKI treatment. We then selected the top ranked 25 genes by a bottleneck algorithm and considered them as critical players in mediating TKI resistance (Figure 2a). *SPHK1* was among these top molecules and may represent a critical player in resistance to TKI treatment (Figure 2b-d). Other interacting genes associated with SPHK1 include filamin B (FLNB), Fos-related antigen 1(FOSL), and stanniocalcin 1 (STC1). It is important to note that *SPHK2* was not upregulated. This is consistent with the preponderance of work showing that *SPHK1* is oncogenic with expression levels in tumors often correlated with poor patient prognosis.

SPHK is expressed in human clear cell RCC

The transcriptome analysis identified SPHK1 as a potentially relevant pathway in RCC. To study SPHK1 in patients, 12 cases of primary ccRCC cases were identified. For one case, a corresponding lung metastasis from the same patient was also available. Nine of twelve cases (75%) of primary ccRCC showed cytoplasmic SPHK1 expression in tumor cells (Figure 3B, C). Faint SPHK1 positivity was seen in the proximal tubules of the normal kidney (Figure 3A). In the case for which primary and metastasis were available, both the primary (Figure 3C) and the metastasis (Figure 3D) were positive for SPHK1 expression.

Patients with metastatic RCC have elevated plasma S1P

SPHK catalyzes the production of S1P. Thus, plasma S1P was compared in patients with metastatic RCC who were scheduled to initiate systemic therapy with a VEGFR TKI. S1P was measured in 97 individuals (Figure 3, bar graph and supplementary Table 1). S1P levels were significantly higher in RCC patients ($F_{1, 95} = 44.71$, $p < 0.001$). Average S1P concentration was 0.689 ± 0.411 μM for RCC patients versus 0.159 ± 0.127 μM for control patients with measurable S1P.

Sphingomab treatment delays RCC tumor growth

To block S1P signaling *in vivo*, mice bearing 786-O xenografts were treated at 2 dose levels of sphingomab. As shown in Figure 4a, all doses tested slowed tumor growth compared to the vehicle treated tumors. Both long axis and tumor volume were measured and recorded and both means of following tumor growth showed similar results. The number of days to increase by 2mm in long axis was recorded as the smallest measurable increase in tumor size and is longer in the 10mg/kg and the 50mg/kg arms compared to the vehicle treated tumors. This change is similar to parameters followed in patients by Response Evaluation Criteria In Solid Tumors (RECIST) criteria. Vehicle treated tumors increased in volume more quickly than those treated with sphingomab ($F_{2, 16} = 4.228$, $p = 0.034$). Average time to +75%

volume was 8.5 days in the control versus 14.7 and 17.5 days in the 10 mg/kg and 50 mg/kg groups, respectively. Vehicle treated tumors also increased in length more quickly than those treated with sphingomab ($F_{2, 16} = 23.437$, $p < 0.001$) and all pairwise treatments were significantly different. Average time to +2mm was 6.2 days in the control versus 15.3 and 20.5 days in the 10 mg/kg and 50 mg/kg groups, respectively.

To confirm these findings in another model, mice bearing A498 tumors were treated with 50mg/kg sphingomab, vehicle or isotype control antibody. Similar to findings in the 786-O tumor model, and shown in Figure 4b, sphingomab delays tumor growth in the A498 tumor model as measured by either long axis or volume. Vehicle treated tumors increased in volume more quickly than those treated with sphingomab ($F_{2, 12} = 4.244$, $p = 0.040$). Average time to +75% was 7.3 days for untreated tumors, 8.2 days for isotype and 14.3 days for sphingomab treated tumors. The sphingomab group was significantly different from both the untreated ($p = 0.036$) and the isotype ($p = 0.032$). The vehicle treated and isotype groups were not significantly different from each other ($p = 0.786$). Vehicle treated and isotype treated A498 tumors also increased in length more quickly than those treated with sphingomab ($F_{2, 12} = 10.513$, $p = 0.002$). Average time to +2mm was 5.0 days in both the untreated and isotype treatments. Time to +2mm averaged 15.29 days in the sphingomab treated group.

Sphingomab slows tumor growth of sunitinib resistant tumors

Sunitinib treatment slows tumor growth but despite continued treatment, tumors eventually grow and develop resistance to therapy. To study S1P inhibition in sunitinib resistant tumors, mice bearing tumors were treated with sunitinib and when resistance (as defined in Methods) developed, were removed from all therapy for 2 days and then randomized to one of 4 arms: vehicle control, rapamycin, sphingomab, or rapamycin + sphingomab. Rapamycin was used to mirror the current clinical evidence that in patients who develop resistance to VEGFR TKI therapy, mTOR inhibition extends time to progression compared to no treatment(11). As shown in Figure 5, sphingomab slowed the growth of sunitinib resistant tumors.

Tumor length comparisons showed that vehicle treated tumors increased in length more quickly than those treated with sphingomab, rapamycin, or both sphingomab and rapamycin ($F_{3,22} = 4.914$, $p = 0.009$). Average time to +2mm was 6.6 days in the vehicle control. Time to +2mm averaged 17.67 days in the sphingomab group ($p = 0.057$ compared to vehicle) and 18.88 days in the rapamycin group ($p = 0.102$ compared to vehicle). Tumors treated with both sphingomab and rapamycin showed the slowest growth, averaging 30.43 days to reach +2mm ($p = 0.001$ compared to control and 0.044 and 0.049 compared to sphingomab or rapamycin alone).

For tumor volume comparisons, we used 40% increase in tumor volume instead of the 75% used in the other experiments because tumors in some treatment arms grew very slowly and never reached +75%. Differences in tumor volume between vehicle treated tumors and those treated with sphingomab, rapamycin, or both sphingomab and rapamycin were nearly significant ($F_{3, 22} = 2.576$, $p = 0.080$). Average time to +40% was 10.2 days in the control,

17.75 days in the sphingomab group, 20.83 days in the rapamycin group, and 23.29 days in the combination sphingomab and rapamycin group.

Sphingomab reduces tumor blood flow

As S1P is a known angiogenic sphingolipid, we measured the effect of S1P inhibition on tumor blood flow by ASL MRI. Mice treated with either PBS or sphingomab were imaged by ASL MRI at baseline prior to treatment and at day 8-10 after treatment. S1P neutralization with sphingomab led to enhanced reduction in tumor blood flow from baseline to day 8-10 (21.93% reduction for sphingomab vs 5.12% reduction for PBS treatment, p=0.040) (Figure 6 and supplementary Table 2). This is consistent with the hypothesis that S1P is an angiogenic target in RCC.

Discussion

In the setting of RCC, VEGF is one of the most critical survival factors for tumors likely due to defects in the von Hippel Lindau (VHL) tumor suppressor and resultant accumulation of HIF, seen in the majority of patients with clear cell RCC. In line with this, VEGFR inhibition with TKI therapy leads to an anti-angiogenic effect and improved clinical outcomes. However, there remains a great unmet need in treating RCC patients as nearly all patients treated with VEGFR TKIs develop resistance to therapy(39,40). An understanding of the mechanisms responsible for resistance is critical for the design of second and third line therapies. We have previously shown that resistance to VEGFR inhibition is due, in part, to resumption of angiogenesis, despite continued treatment with TKIs(31,32,36). We have also known that the hypoxia which follows initial tumor devascularization produced by anti-VEGF therapy can modulate pathways responsible for acquired resistance(40). Several groups (28,41,42) have invoked an association between upregulation of key HIF proteins in the hypoxic tumor microenvironment and SPHK1 expression to explain the contribution of S1P production to tumor growth and treatment resistance. (43,44)

Because of the well-known SPHK1-HIF axis associated with hypoxia and resistance in the context of prostate and other cancers (42,43,45), we hypothesized that the resistance to VEGFR TKI therapy in mice bearing human RCC tumors and patients with RCC would show an upregulation of the SPHK1/S1P signaling system. Accordingly, we found that mice bearing human RCC tumors showed an upregulation of several hypoxia-related genes, including *SPHK1*. Upregulation of *SPHK1* and its interactants was seen in 3 treatment contexts and network analysis identified SPHK as a master regulator molecule. In addition, we demonstrated for the first time that patients with RCC show SPHK1 expression in their tumors and elevated plasma S1P levels. These data support the hypothesis that an anti-S1P therapy would be beneficial after VEGFR TKI failure and that the SPHK1/S1P signaling system could contribute to VEGFR TKI resistance. Sphingosine Kinase 1 (SPHK1) is up-regulated in many solid tumor types (18–25,46). For ovarian, glioblastoma, breast and other cancer types, SPHK1 expression correlated with mortality in patients (18,20,21,23,26,27). This is to our knowledge, the first study to demonstrate SPHK1 expression in RCC.

We tested the anti-tumor activity of murine anti-S1P mAb, sphingomab, as a first line therapy and second line therapy in sequence with sunitinib. In both settings, sphingomab

inhibited tumor progression. These data place S1P inhibition in two spaces of clinical testing. The effects seen in both the treatment naïve setting and after VEGFR TKI resistance could be a result of the overall susceptibility of RCC to S1P inhibition in addition to its role in resistance. Importantly, the combination of sphingomab and mTOR inhibition with rapamycin resulted in some additive benefit, and merits further exploration.

To date, multiple experimental findings support the role of S1P as a promoter of tumor growth, angiogenesis, chemoresistance and metastasis. Sphingomab is the first monoclonal therapeutic antibody that works as a molecular sponge for extracellular S1P, blocking its biological activities through all S1P receptors on tumor cells and the tumor microenviroment. Based on the result presented, the inhibition of S1P signaling using the anti-S1P antibody approach may represent a novel approach to addressing VEGFR TKI failures in the human RCC setting. In our models, sphingomab appears to have an antiangiogenic effect as evidenced by reduced ASL MRI measured tumor blood flow. Our prior studies have shown that treatment with sunitinib results in a 50-80% reduction in tumor blood flow from baseline(33,47). S1P inhibition lowers perfusion to a lesser magnitude. Thus, we hypothesize that anti-S1P exerts either an effect on vessel function beyond flow and /or angiogenic independent effects.However, in general, the efficacy and anti angiogenic effects of sphingomab in the renal cancer models is in line with effects of anti-S1P therapy shown in other animal models of human tumors(14).

In the current study, we identified the S1P pathway as relevant in patients with RCC as plasma levels were elevated in patients with metastatic RCC vs. healthy volunteers. S1P may represent a biomarker for selection of patients who might benefit from S1P pathway inhibitors. Assays to detect free and bound S1P are currently being developed for this purpose and may help guide future trials. Decrease in lymphocyte counts has also been reported to be a biomarker for S1P pathway inhibition supporting a potential immunomodulatory role for S1P inhibitors(48,49). Future studies will also help define the specific effects of S1P on tumor immunity. We also detected expression of SPHK1 in most primary RCC tumors and concordant expression in one metastatic lesion. SPHK1 expression may be another marker for response to S1P pathway inhibition and we are conducting further studies to assess SPHK1 expression in relation to tumor grade and clinical outcome in primary tumors and metastases.

Concurrent with our studies, the humanized form of the anti-S1P mAb, sonepcizumab/ ASONEP™, was developed for clinical testing. A Phase I safety study was recently completed for sonepcizumab. The ASONEP trial was a multi-center, open-label, single-arm, dose escalation study of sonepcizumab administered as a single agent weekly to subjects with refractory advanced solid tumors at doses between 1 and 24 mg/kg (50). Sonepcizumab was well tolerated with no dose-limiting toxicities observed. Based on this study and our preclinical studies, a Phase II trial is underway in patients with RCC who have progressed following VEGFR TKI treatment.

Future studies will focus on the specific mechanisms by which S1P pathway blockade slows tumor growth. Additionally, biomarkers of response and resistance to S1P pathway

inhibition may help guide the clinical development of this new therapeutic option for patients with RCC.

Supplementary Material

Refer to Web version on PubMed Central for supplementary material.

Acknowledgments

Support: This work was supported by research grants awarded to RB from the National Institutes of Health/ National Cancer Institute (5K08CA138900) and the Dana-Farber/Harvard Cancer Center Kidney SPORE National Cancer Institute (P50CA101942-08and to RS from the National Institutes of Health/National Cancer Institute (R44CA110298)

References

1. Jemal A, Siegel R, Ward E, Hao Y, Xu J, Thun MJ. Cancer Statistics , 2009. CA Cancer J Clin. 2009; 59:225–49. [PubMed: 19474385]
2. Lam JS, Leppert JT, Belldegrun AS. Figlin R a. Novel approaches in the therapy of metastatic renal cell carcinoma. World J Urol. 2005; 23:202–12. [PubMed: 15812574]
3. Janzen NK, Kim HL, Figlin RA, Belldegrun AS. Surveillance after radical or partial nephrectomy for localized renal cell carcinoma and management of recurrent disease. Urol Clin North Am. 2003; 30:843–52. [PubMed: 14680319]
4. Escudier B, Eisen T, Stadler W, Szczylik C, Oudard S, Staehler M, et al. Sorafenib for treatment of renal cell carcinoma: Final efficacy and safety results of the phase III treatment approaches in renal cancer global evaluation trial. J Clin Oncol. 2009; 27:3312–8. [PubMed: 19451442]
5. Motzer R, Hutson T, Tomczak P, Michaelson M, Bukowski R, Oudard S, et al. Overall survival and updated results for sunitinib compared with interferon alfa in patients with metastatic renal cell carcinoma. J Clin Oncol. 2009; 27:3584–90. [PubMed: 19487381]
6. Rini B, Escudier B, Tomczak P, Kaprin A, Szczylik C, Hutson T, et al. Comparative effectiveness of axitinib versus sorafenib in advanced renal cell carcinoma (AXIS): a randomised phase 3 trial. Lancet. 2011; 378:1931–9. [PubMed: 22056247]
7. Sternberg C, Davis I, Mardiak J, Szczylik C, Lee E, Wagstaff J, et al. Pazopanib in locally advanced or metastatic renal cell carcinoma: results of a randomized phase III trial. J Clin Oncol. 2010; 28:1061–8. [PubMed: 20100962]
8. Motzer; Hutson, Robert J.; McCann, Thomas E.; Lauren Choueiri, TK. Overall Survival in Renal-Cell Carcinoma with Pazopanib versus Sunitinib. N Engl J Med. 2014; 370:1769–70. [PubMed: 24785224]
9. Procopio G, Verzoni E, Bracarda S, Ricci S, Sacco C, Ridolfi L, et al. Overall survival for sorafenib plus interleukin-2 compared with sorafenib alone in metastatic renal cell carcinoma (mRCC): final results of the ROSORC trial. Ann Oncol. 2013; 24:2967–71. [PubMed: 24063860]
10. Hudes G, Carducci M, Tomczak P, Dutcher J, Figlin R, Kapoor A, et al. Temsirolimus, interferon alfa, or both for advanced renal-cell carcinoma. N Engl J Med. 2007; 356:2271–81. [PubMed: 17538086]
11. Motzer R, Escudier B, Oudard S, Hutson T, Porta C, Bracarda S, et al. Efficacy of everolimus in advanced renal cell carcinoma: a double-blind, randomised, placebo-controlled phase III trial. Lancet. 2008; 372:449–56. [PubMed: 18653228]
12. Sabbadini, R a. Sphingosine-1-phosphate antibodies as potential agents in the treatment of cancer and age-related macular degeneration. Br J Pharmacol. 2011; 162:1225–38. [PubMed: 21091645]
13. Lee MJ, Thangada S, Claffey KP, Ancellin N, Liu CH, Kluk M, et al. Vascular endothelial cell adherens junction assembly and morphogenesis induced by sphingosine-1-phosphate. Cell. 1999; 99:301–12. [PubMed: 10555146]

14. Visentin B, Vekich JA, Sibbald BJ, Cavalli AL, Moreno KM, Matteo RG, et al. Validation of an anti- sphingosine-1-phosphate antibody as a potential therapeutic in reducing growth, invasion, and angiogenesis in multiple tumor lineages. Cancer Cell. 2006; 9:225–38. [PubMed: 16530706]
15. Takuwa Y, Okamoto H, Takuwa N, Gonda K, Sugimoto N, Sakurada S. Subtype-specific, differential activities of the EDG family receptors for sphingosine-1-phosphate, a novel lysophospholipid mediator. Mol Cell Endocrinol. 2001; 177:3–11. [PubMed: 11377814]
16. Xia P, Gamble JR, Wang L, Pitson SM, Moretti PAB, Wattenberg BW, et al. An oncogenic role of sphingosine kinase. Curr Biol. 2000; 10:1527–30. [PubMed: 11114522]
17. Pyne NJ, Pyne S. Sphingosine 1-phosphate and cancer. Nat Rev Cancer. Nature Publishing Group. 2010; 10:489–503.
18. Long JS, Edwards J, Watson C, Tovey S, Mair KM, Schiff R, et al. Sphingosine kinase 1 induces tolerance to human epidermal growth factor receptor 2 and prevents formation of a migratory phenotype in response to sphingosine 1-phosphate in estrogen receptor-positive breast cancer cells. Mol Cell Biol. 2010; 30:3827–41. [PubMed: 20516217]
19. Ruckhäberle E, Rody A, Engels K, Gaetje R, von Minckwitz G, Schiffmann S, et al. Microarray analysis of altered sphingolipid metabolism reveals prognostic significance of sphingosine kinase 1 in breast cancer. Breast Cancer Res Treat. 2008; 112:41–52. [PubMed: 18058224]
20. Li W, Yu C-P, Xia J, Zhang L, Weng G-X, Zheng H, et al. Sphingosine kinase 1 is associated with gastric cancer progression and poor survival of patients. Clin Cancer Res. 2009; 15:1393–9. [PubMed: 19228740]
21. Van Brocklyn JR, Jackson C a, Pearl DK, Kotur MS, Snyder PJ, Prior TW. Sphingosine kinase-1 expression correlates with poor survival of patients with glioblastoma multiforme: roles of sphingosine kinase isoforms in growth of glioblastoma cell lines. J Neuropathol Exp Neurol. 2005; 64:695–705. [PubMed: 16106218]
22. Pyne S, Edwards J, Ohotski J, Pyne NJ. Sphingosine 1-phosphate receptors and sphingosine kinase 1: novel biomarkers for clinical prognosis in breast, peostate, and hematological cancers. 2012; 2:1–5.
23. Dayon A, Brizuela L, Martin C, Mazerolles C, Pirot N, Doumerc N, et al. Sphingosine Kinase-1 Is Central to Androgen-Regulated Prostate Cancer Growth and Survival. PLoS One. 2009:4.
24. Brünnert D, Sztachelska M, Bornkessel F, Treder N, Wolczynski S, Goyal P, Zygmunt M. Lysophosphatidic acid and Sphingosine 1-phosphate metabolic pathways and their receptors are differentially regulated during decidualization of human endometrial stromal cells. Mol Hum Reprod. 2014; 20:1016–25. [PubMed: 24994816]
25. Yang Y, Ji C, Cheng L, He L, Lu C, Wang R, et al. Sphingosine kinase-1 inhibition sensitizes curcumin- induced growth inhibition and apoptosis in ovarian cancer cells. Cancer Sci. 2012; 103:1538–45. [PubMed: 22594559]
26. Meng X-D, Zhou Z-S, Qiu J-H, Shen W-H, Wu Q, Xiao J. Increased SPHK1 expression is associated with poor prognosis in bladder cancer. Tumour Biol. 2014; 35:2075–80. [PubMed: 24092575]
27. Ruckhäberle E, Karn T, Denkert C, Loibl S, Ataseven B, Reimer T, et al. Predictive value of sphingosine kinase 1 expression in neoadjuvant treatment of breast cancer. J Cancer Res Clin Oncol. 2013; 139:1681–9. [PubMed: 23955546]
28. Cuvillier O, Ader I, Bouquerel P, Brizuela L, Malavaud B, Mazerolles C, et al. Activation of sphingosine kinase-1 in cancer: implications for therapeutic targeting. Curr Mol Pharmacol. 2010; 3:53–65. [PubMed: 20302564]
29. Raguz S, Yague E. Resistance to chemotherapy: new treatments and novel insights into an old problem. Br J Cancer. 2008; 99:387–91. [PubMed: 18665178]
30. O'Brien N, Jones ST, Williams DG, Cunningham HB, Moreno K, Visentin B, et al. Production and characterization of monoclonal anti-sphingosine-1-phosphate antibodies. J Lipid Res. 2009; 50:2245–57. [PubMed: 19509417]
31. Bhatt R, Wang X, Zhang L, Collins M, Signoretti S, Alsop D, et al. Renal cancer resistance to antiangiogenic therapy is delayed by restoration of angiostatic signaling. Mol Cancer Ther. 2010; 9:2793–802. [PubMed: 20699227]

32. Zhang L, Bhasin M, Schor-Bardach R, Wang X, Collins M, Panka D, et al. Resistance of renal cell carcinoma to sorafenib is mediated by potentially reversible gene expression. PLoS One. 2011; 6:e19144. [PubMed: 21559452]
33. Wang X, Zhang L, O'Neill A, Bahamon B, Alsop D, Mier J, et al. Cox-2 inhibition enhances the activity of sunitinib in human renal cell carcinoma xenografts. Br J Cancer. 2013; 108:319–26. [PubMed: 23322198]
34. Gentleman, Robert; Vincent, J.; Carey; Huber, Wolfgang; Rafael, A.; Irizarry, SD. Bioinformatics and Computational Biology Solutions Using R and Bioconductor. Springer; New York: 2005. p. 397-420.
35. Bhasin MK, Dusek J a, Chang B-H, Joseph MG, Denninger JW, Fricchione GL, et al. Relaxation response induces temporal transcriptome changes in energy metabolism, insulin secretion and inflammatory pathways. PLoS One. 2013; 8:e62817. [PubMed: 23650531]
36. Schor-Bardach R, Alsop D, Pedrosa I, Solazzo S, Wang X, Marquis R, et al. Does arterial spin-labeling MR imaging-measured tumor perfusion correlate with renal cell cancer response to antiangiogenic therapy in a mouse model? Radiology. 2009; 251:731–42. [PubMed: 19474376]
37. Alsop D, Detre J. Reduced transit-time sensitivity in noninvasive magnetic resonance imaging of human cerebral blood flow. J Cereb blood flow Metab. 1996; 16:1236–49. [PubMed: 8898697]
38. Murate T, Banno Y, T-Koizumi K, Watanabe K, Mori N, Wada A, et al. Cell Type-specific Localization of Sphingosine Kinase 1a in Human Tissues. J Histochem Cytochem. 2001; 49:845–55. [PubMed: 11410609]
39. Rini BI, Atkins MB. Resistance to targeted therapy in renal-cell carcinoma. Lancet Oncol. 2009; 10:992–1000. [PubMed: 19796751]
40. Bergers G, Hanahan D. Modes of resistance to anti-angiogenic therapy. Nat Rev Cancer. 2008; 8:592–603. [PubMed: 18650835]
41. Brizuela L, Ader I, Mazerolles C, Bocquet M, Malavaud B, Cuvillier O. First evidence of sphingosine 1-phosphate lyase protein expression and activity downregulation in human neoplasm: implication for resistance to therapeutics in prostate cancer. Mol Cancer Ther. 2012; 11:1841–51. [PubMed: 22784711]
42. Anelli V, Gault CR, Cheng AB, Obeid LM. Sphingosine kinase 1 is up-regulated during hypoxia in U87MG glioma cells. Role of hypoxia-inducible factors 1 and 2. J Biol Chem. 2008; 283:3365–75. [PubMed: 18055454]
43. Cuvillier O, Ader I, Bouquerel P, Brizuela L, Gstalder C, Malavaud B. Hypoxia, therapeutic resistance, and sphingosine 1-phosphate. Adv Cancer Res. 2013; 117:117–41. [PubMed: 23290779]
44. Ader I, Brizuela L, Bouquerel P, Malavaud B, Cuvillier O. Sphingosine kinase 1: a new modulator of hypoxia inducible factor 1alpha during hypoxia in human cancer cells. Cancer Res. 2008; 68:8635–42. [PubMed: 18922940]
45. Johnson KR, Johnson KY, Becker KP, Bielawski J, Mao C, Obeid LM. Role of human sphingosine-1- phosphate phosphatase 1 in the regulation of intra- and extracellular sphingosine-1-phosphate levels and cell viability. J Biol Chem. 2003; 278:34541–7. [PubMed: 12815058]
46. Song L, Xiong H, Li J, Liao W, Wang L, Wu J, et al. Sphingosine kinase-1 enhances resistance to apoptosis through activation of PI3K/Akt/NF-κB pathway in human non-small cell lung cancer. Clin cancer Res. 2011; 17:1839–49. [PubMed: 21325072]
47. Wang, X.; Bullock, AJ.; Zhang, L.; Wei, L.; Yu, D.; Mahagaokar, K., et al. The role of angiopoietins as potential therapeutic targets in renal cell carcinoma. Transl Oncol. Vol. 7. Neoplasia Press, Inc.; 2014. p. 188-95.
48. Gräler MH. Cellular Physiology and Biochemistr y Biochemistry Targeting Sphingosine 1-phosphate (S1P) Levels and S1P Receptor Functions for Therapeutic Immune Interventions. Cell Physiol Biochem. 2010; 26:79–86. [PubMed: 20502007]
49. Pham THM, Baluk P, Xu Y, Grigorova I, Bankovich AJ, Pappu R, et al. Lymphatic endothelial cell sphingosine kinase activity is required for lymphocyte egress and lymphatic patterning. J Exp Med. 2010; 207:17–27. [PubMed: 20026661]

50. Gordon MS, Just R, Rosen LS DA. A phase I study of sonepcizumab (S), a humanized monoclonal antibody to sphingosine-1-phosphate (S1P), in patients with advanced solid tumors. J Clin Oncol. 2010; 28(15S Part 1 of 2):219s.

Translational Relevance

Vascular endothelial growth factor (VEGF) pathway inhibition can be efficacious in metastatic renal cell carcinoma (RCC), but resistance to therapy is a clinical problem. This study shows that VEGF receptor inhibition in murine models leads to upregulation of sphingosine kinase 1 (SPHK1) and bioinformatics analyses indicate that SPHK1 may be a central signaling pathway in RCC. SPHK1 catalyzes the production of the bioactive sphingolipid, sphingosine -1- phosphate (S1P). SPHK1 is expressed in human RCC and S1P is present in RCC patient plasma. In vivo, S1P inhibition with a neutralizing antibody, sphingomab, slows tumor growth in murine RCC. Efficacy is seen in treatment naïve tumor models and also after VEGF receptor inhibition. This study provides the preclinical evidence for testing of S1P pathway inhibition in metastatic RCC.

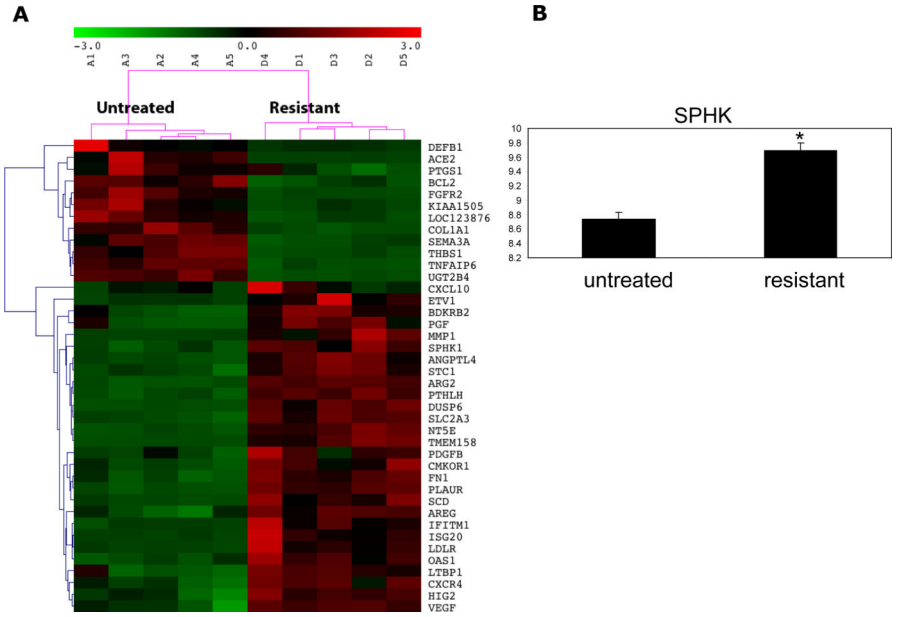

Figure 1.

Heatmap depicting transcripts that are differentially expressed in untreated vs sorafenib resistant murine 786-O tumors is shown. The columns represent the samples and rows represent the genes. Gene expression is shown with pseudocolor scale (-3 to 3) with red denoting high expression level and green denoting low expression (A). RT-PCR for *SPHK1* is shown in B and is elevated in resistant tumors vs untreated tumors (P=0.005).

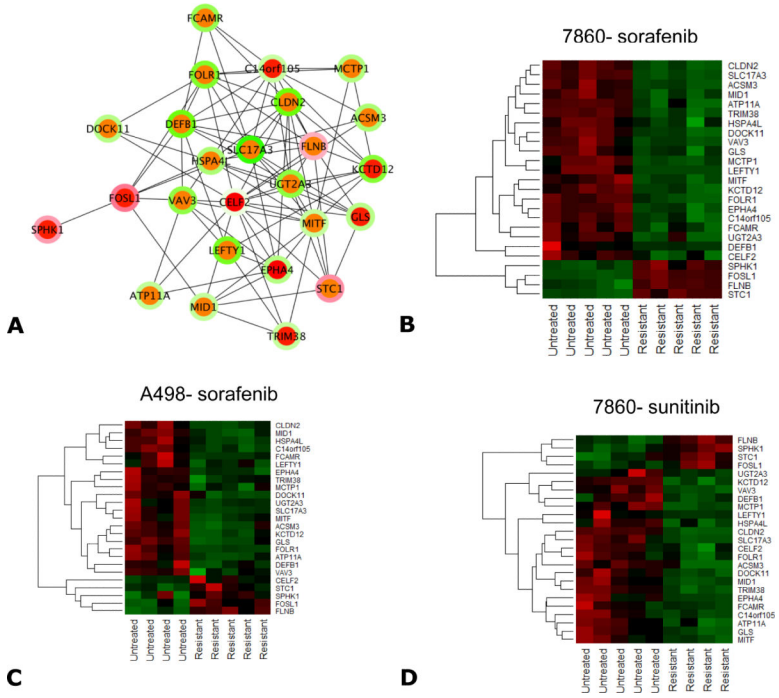

Figure 2.

A systems biology oriented analysis of the 75 commonly differentially expressed genes from 786-O tumors treated with sorafenib or sunitinib and A498 tumors treated with sorafenib is shown. Panel A shows the interactive network of the top 25 bottleneck molecules liked to the resistant phenotype. Each node specifies a gene and the color at the node edges represents the interactions. The inner color of each node indicates the bottleneck rank (red indicates higher ranking and green indicates lower ranking) which signifies criticality in maintaining the stability of the network. The outer ring of the node indicates the fold change comparing the untreated vs resistant samples. Upregulation or downregulation are shown by red and green respectively. (B-D) Heatmaps of the 25 bottleneck molecules linked to resistance in the 3 treated conditions (786-O sorafenib, 786-O sunitinib, and A498 sorafenib). In the heatmaps, columns represent tumor samples and rows represent genes. The expression is shown using a pseudocolor scale (-1 to +1 with upregulation or downregulation shown by red and green respectively).

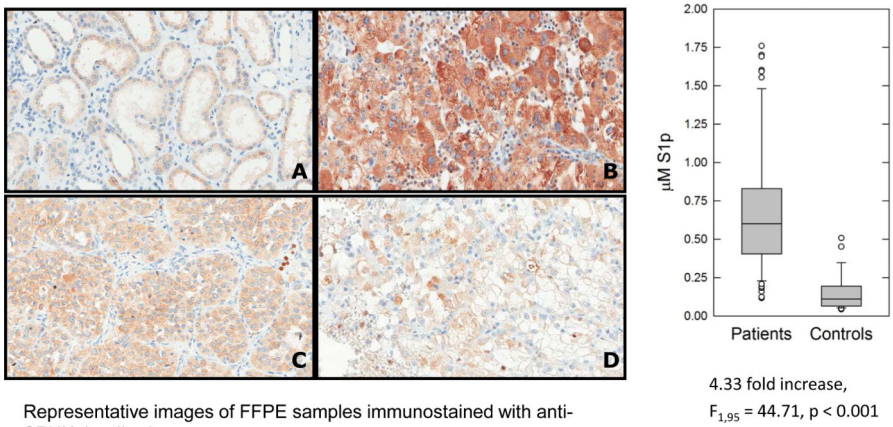

Representative images of FFPE samples immunostained with anti-SPHK-1antibody.
(A) Positive normal proximal kidney tubules,
(B) Positive primary ccRCC,
(C) Positive primary ccRCC (D) positive corresponding lung metastasis from same pt.

Figure 3.

SPHK1 expression was assessed by immunohistochemistry in 12 cases of primary RCC. Representative images are shown: (A) Positive normal proximal kidney tubules, (B) Positive primary ccRCC, (C) Positive primary ccRCC (B and C represent independent cases) and (D) positive corresponding lung metastasis (same patient as C).

Plasma S1P was measured in patients with metastatic RCC (n=69) vs healthy controls (n=28) (bar graph). S1P levels were significantly higher in RCC patients ($F_{1, 95} = 44.71$, *$p < 0.001$). Average S1P concentration was 0.689 ± 0.411 mM for RCC patients versus 0.159 ± 0.127 mM for healthy volunteers. S1P was initially measured in 110 individuals. 13 individuals in the control group had S1P levels that were too low to be reliably quantified by the assay. To be conservative, these individuals were excluded from the analysis.

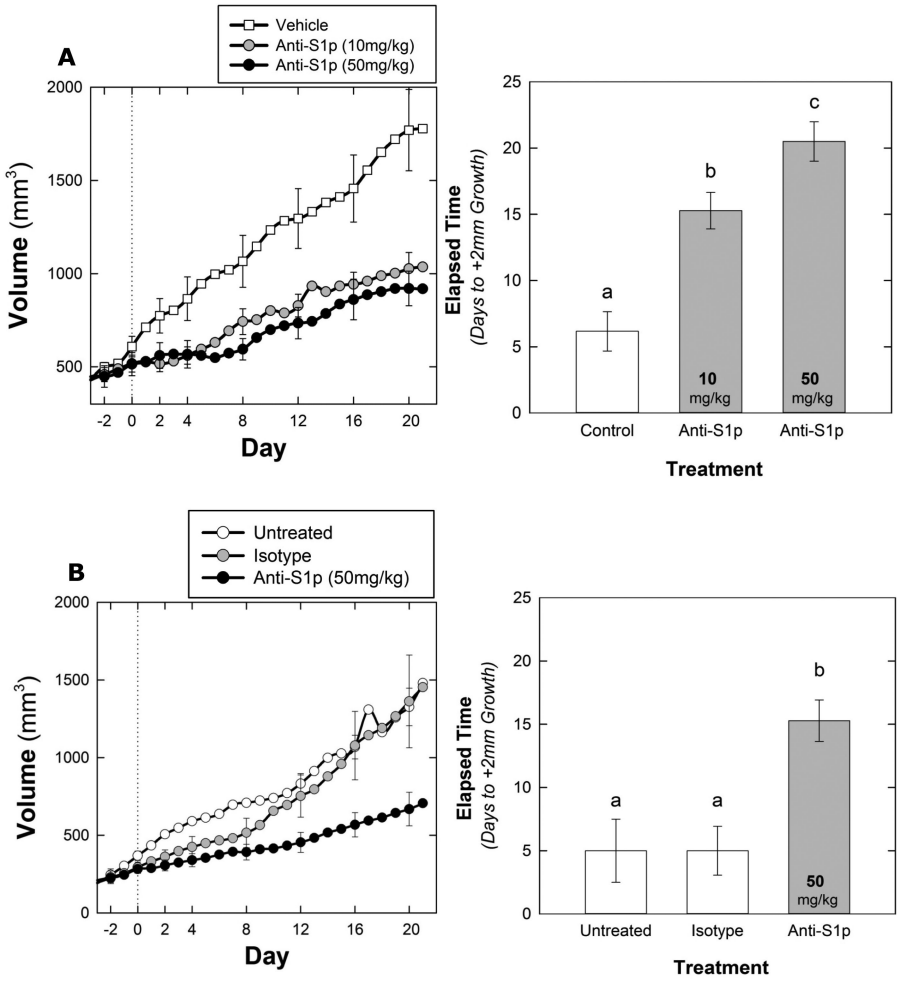

Figure 4.

Growth curves depicting average tumor volume of 786-O (A) derived tumors from mice treated with vehicle gavage (n = 6), sphingomab (10 mg/kg, n=7) (A), sphingomab (50 mg/kg, n=6). A (left) Vehicle treated tumors increased in volume more quickly than those treated with sphingomab ($F_{2, 16} = 4.228$, $p = 0.034$). Average time to +75% volume was 8.5 days in the control versus 14.7 and 17.5 days in the 10 mg/kg and 50 mg/kg groups, respectively. (right) Control tumors increased in length more quickly than those treated with sphingomab ($F_{2, 16} = 23.437$, $p < 0.001$) and all pairwise treatments were significantly different. Average time to +2mm was 6.2 days in the control versus 15.3 and 20.5 days in the 10 mg/kg and 50 mg/kg groups, respectively.

(B)Tumor growth in the A498 model is shown (left) vehicle treated tumors increased in volume more quickly than those treated with sphingomab ($F_{2, 12} = 4.244$, $p = 0.040$). Average time to +75% was 7.3 days for untreated tumors (n = 3), 8.2 days for isotype treated (n = 5) and 14.3 days for sphingomab treated tumors. The sphingomab group was significantly different from both the vehicle treated ($p = 0.036$) and the isotype control treated ($p = 0.032$). The vehicle and isotype treated groups were not significantly different from each other ($p = 0.786$)

(Right) Vehicle and isotype tumors increased in length more quickly than those treated with sphingomab ($F_{2, 12} = 10.513$, $p = 0.002$). Average time to +2mm was 5.0 days in both the vehicle and isotype treatments (n = 5 and 3 respectively). Time to +2mm averaged 15.29 days in the sphingomab group (n = 7).

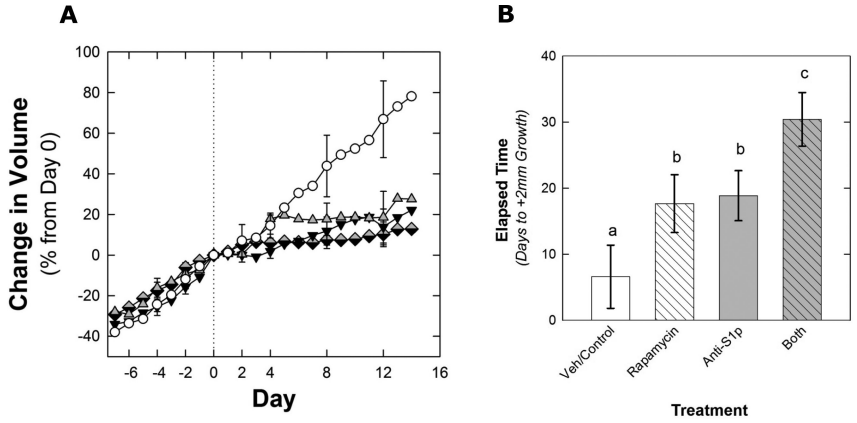

Figure 5.

Growth curves depicting average tumor volume of 786-O–derived tumors from mice treated initially with sunitinib then switched to either vehicle (n = 6), sphingomab (50 mg/kg, n=5), rapamycin (n = 8), sphingomab (50 mg/kg), plus rapamycin (n=7). A 2 day treatment washout was initiated after the tumors developed resistance to sunitinib (growth by +2mm in long axis) and then the second treatment regimen was started. (A) Differences in tumor volume between vehicle treated tumors and those treated with sphingomab, rapamycin, or both sphingomab and rapamycin were nearly significant ($F_{3, 22} = 2.576$, $p = 0.080$). Average time to +40% was 10.2 days in the control, 17.75 days in the sphingomab, 20.83 days in the rapamycin group, and 23.29 days in the combination sphingomab and rapamycin group (B). Vehicle treated tumors increased in length more quickly than those treated with sphingomab, rapamycin, or both sphingomab and rapamycin ($F_{3, 22} = 4.914$, $p = 0.009$). Average time to +2mm was 6.6 days in the control. Time to +2mm averaged 17.67 days in the sphingomab group (n = 6, p = 0.057) and 18.88 days in the rapamycin group (p = 0.102). Tumors treated with both sphingomab and rapamycin grew the least, averaging 30.43 days to reach +2mm (p = 0.001 compared to control and 0.044 and 0.049 compared to sphingomab or rapamycin alone).

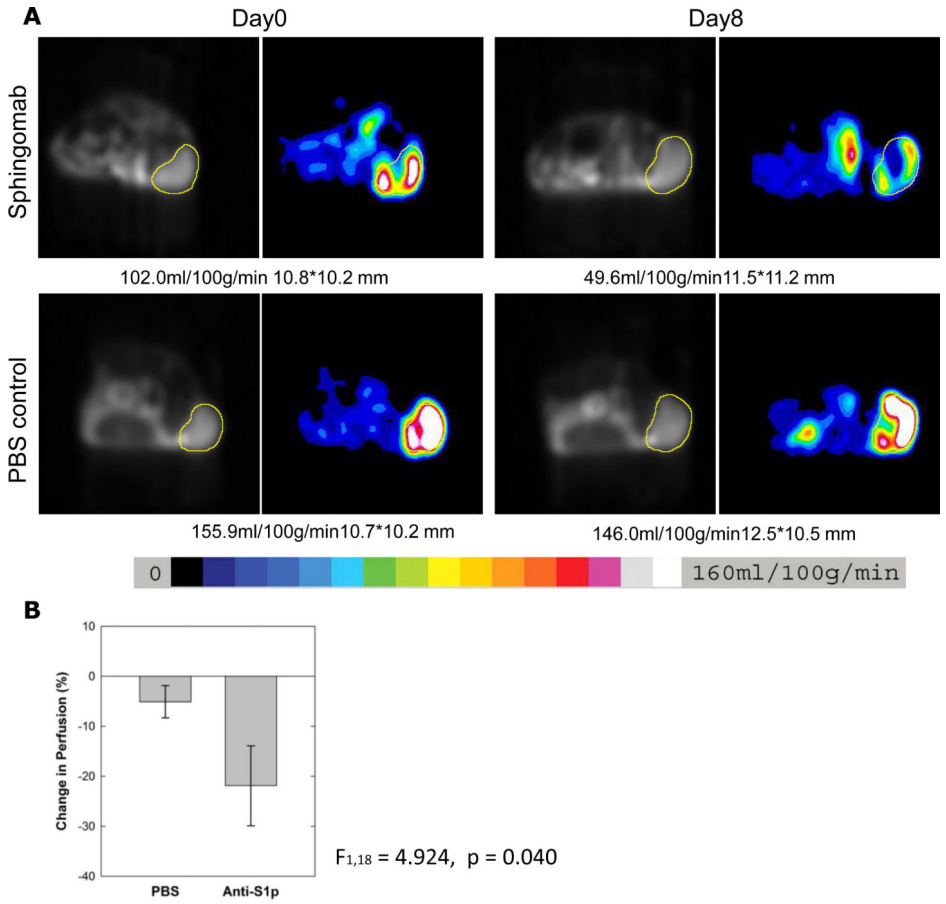

Figure 6.

ASL MRI tumor perfusion of representative tumors treated with vehicle (PBS, n=12) vs sphingomab (n=8) (A). The tumor is indicated by the region of interest outlined in yellow and the color scale is shown. (B), tumor perfusion after 8 days of therapy is reduced in the sphingomab treatment group vs the vehicle (PBS) (p=0.04).